Heterogeneity of morphometric similarity networks in health and schizophrenia

Joost Janssen[1,2,±,*], Ana Guil Gallego[1,*], Covadonga M. Díaz-Caneja[1,2,3], Noemi González Lois[1], Niels Janssen[4,5,6], Javier González-Peñas[1,2], Pedro M. Gordaliza[7,8], Elizabeth E.L. Buimer[9], Neeltje E.M. van Haren[9,10], Celso Arango[1,2,3], René S. Kahn[9,11], Hilleke E. Hulshoff Pol[9] & Hugo G. Schnack[9,10,12]

[1]Department of Child and Adolescent Psychiatry, Institute of Psychiatry and Mental Health, Hospital General Universitario Gregorio Marañón, Instituto de Investigación Sanitaria Gregorio Marañón (IiSGM), Madrid, Spain.
[2]Ciber del Área de Salud Mental (CIBERSAM), Instituto de Salud Carlos III, Madrid, Spain.
[3]School of Medicine, Universidad Complutense, Madrid, Spain.
[4]Department of Psychology, Universidad de la Laguna, Tenerife, Spain.
[5]Institute of Biomedical Technologies, Universidad de La Laguna, Tenerife, Spain.
[6]Institute of Neurosciences, Universidad de la Laguna, Santa Cruz de Tenerife, Spain.
[7]CIBM Center for Biomedical Imaging, Lausanne, Switzerland
[8]Radiology Department, Lausanne University Hospital (CHUV) and University of Lausanne, Lausanne, Switzerland
[9]Department of Psychiatry, UMCU Brain Center, University Medical Center Utrecht, Utrecht, The Netherlands.
[10]Department of Child and Adolescent Psychiatry/Psychology, Erasmus University Medical Centre, Sophia Children's Hospital, Rotterdam, The Netherlands.
[11]Department of Psychiatry, Icahn School of Medicine at Mount Sinai, New York, United States.
[12]Department of Languages, Literature, and Communication, Faculty of Humanities, Utrecht University, Utrecht, The Netherlands
[±]Corresponding author
[*]Contributed equally

Word count abstract:
Word count text body:
Short title:
Figures: Embedded in text body
Tables:

Correspondence to:
Joost Janssen, PhD
Department of Child and Adolescent Psychiatry
Hospital General Universitario Gregorio Marañón
C/ Ibiza, 43. 28009-Madrid, Spain
Phone: 0034914265005
Fax: 0034914265004
Mail: joost.janssen76@gmail.com

Abstract

Introduction

Morphometric similarity is a recently developed neuroimaging phenotype of inter-regional connectivity by quantifying the similarity of a region to other regions based on multiple MRI parameters assessed at each region. At the group-level, altered average morphometric similarity has been reported in psychotic disorders. At the individual level variability of morphometric similarity exists. We used normative modeling to address inter-individual heterogeneity of morphometric similarity in health and schizophrenia.

Methods

Morphometric similarity for 68 cortical regions were obtained from baseline and follow-up T1-weighted scans of healthy individuals and patients with chronic schizophrenia. Using Bayesian Linear Regression and taking into account age, sex, image quality and scanner, normative models were trained and validated in healthy controls from multi-site data (n = 4310). Individual deviations from the norm (z-scores) were computed for each participant for each region at both timepoints. A z-score ≧ than 1.96 was considered supra-normal and a z-score ≦ -1.96 infra-normal. As a longitudinal metric we calculated the change over time of the total number of infra- or supra-normal regions per participant. Regions were classified into seven predefined brain networks that have been derived from resting state functional MRI in order to assess morphometric similarity of functional networks.

Results

The percentage of patients with infra- or supra-normal values for any region at baseline and follow-up was low (<6%) and not different from healthy controls. There were no longitudinal group differences in change over time of the total number of

infra- or supra-normal regions per participant. At baseline, patients had decreased morphometric similarity of the default mode network and increased morphometric similarity of the somatomotor network when compared to healthy controls.

Conclusions

In a case-control setting, a decrease of morphometric similarity within the default mode network may be a robust finding implicated in schizophrenia. Nevertheless, significant reductions were evident only in a minority of patients indicating that caution is warranted when extrapolating group-average results to the individual.

Introduction

Schizophrenia is a debilitating psychiatric disorder that afflicts a significant percentage of the global population, with its prevalence estimated at an approximate percentage of 1% (McGrath et al., 2008). A considerable challenge hindering the development of more effective, personalized treatment strategies for schizophrenia lies in the unresolved neurobiological heterogeneity that characterizes the disease (Brugger and Howes, 2017; Alnæs et al., 2019). While morphological reductions in brain volume and cortical thickness may be relatively robust at the group level, their individual manifestations exhibit considerable variation across individuals with schizophrenia (Haijma et al., 2013; Brugger and Howes, 2017; Kelly et al., 2018; van Erp et al., 2018; Segal et al., 2023). Consequently, it is important to leverage new methods that facilitate a deeper understanding of this heterogeneity.

To address the issue of phenotypic heterogeneity, a recent methodological development known as the normative modeling framework has been proposed. This framework offers the potential to account for the unique neurobiological profiles of individuals by establishing normative standards and subsequently assessing each individual's deviation from these norms (Marquand et al., 2019). Cross-sectional studies applying normative model analysis in schizophrenia are sparse but have shown that abnormal deviations of regional cortical thickness and volume are frequent at the individual level but rarely occur consistently in the same locations and with the same severity across individuals (Wolfers et al., 2018; Lv et al., 2021; Di Biase et al., 2022; Segal et al., 2023). To the best of our knowledge, there are no longitudinal normative modeling studies in individuals with chronic schizophrenia which enable assessment of intra-individual change in deviation between two

timepoints and its relation to the established normative range (Di Biase et al., 2023; Barbora Rehák Bučková et al., 2024).

Morphometric similarity is a recently developed neuroimaging phenotype of cortical inter-regional connectivity by quantifying the similarity of a region to all other regions based on multiple MRI parameters assessed at each region (Seidlitz et al., 2018; Sebenius et al., 2023). That is, each brain region is represented as a vector of several MRI features, such as cortical thickness and volume, and based on the pairwise correlation between the regional feature vectors, morphometric similarity can be estimated. One study found that regions with high morphometric similarity also had stronger axonal connectivity, providing support for morphometric similarity as a proxy for inter-regional connectivity (Seidlitz et al., 2018). Morphometric similarity has shown promise as a marker of psychosis as reduced average morphometric similarity in frontal and temporal regions replicated in three independent groups of adult patients with psychosis and one group of individuals with early-onset schizophrenia (Morgan et al., 2019; Yao et al., 2023). In addition, a disproportionate number of regions that showed group-average reductions in morphometric similarity in individuals with psychosis were part of the default mode network (Morgan et al., 2019). This finding fits with the notion that psychosis may be associated with altered connectivity across regions that belong to the default mode network (Broyd et al., 2009; Heuvel and Sporns, 2019). However, it is worth noting that diagnostic investigations into morphometric similarity have predominantly relied on group-level averages, thereby overlooking potentially substantial heterogeneity of morphometric similarity at the individual level (Morgan et al., 2019; Zhukovsky et al., 2022; Yao et al., 2023).

The current study uses normative modeling to establish normative morphometric similarity using a large sample of healthy controls (n=4310). Thereafter, we aim to assess and decompose the heterogeneity of morphometric similarity of seven widely recognized functional networks in a longitudinal sample of adult individuals with schizophrenia and healthy controls.

Methods

Sample

Eleven datasets were combined to create the full sample. These datasets are described in Figure A including the sample size, age, and sex distribution of each dataset. Ten datasets are publicly available and either include healthy individuals only or only healthy individuals from the baseline datasets were included for the current study: the Amsterdam Open MRI Collection (aomic) (id1000, piop1 and piop2) datasets (Snoek et al., 2021), the Cambridge Centre for Ageing and Neuroscience (camcan) dataset (Shafto et al., 2014), the Dallas Longitudinal Brain Study (dlbs) dataset (Lu et al., 2011), the Information eXtraction from Images (ixi) dataset (http://brain-development.org/ixidataset/), the Narratives (narratives) dataset (Nastase et al., 2021), the Open Access Series of Imaging Studies (oasis3) dataset (Marcus et al., 2010), the NKI-Rockland (rockland) dataset (Nooner et al., 2012) and the Southwest University adult lifespan (sald) dataset (Wei et al., 2018). One dataset is not publicly available and consisted of a large longitudinal sample of individuals with schizophrenia and healthy participants aged 16-68 years (at baseline) from the Utrecht Schizophrenia project and the Genetic Risk and Outcome of Psychosis (GROUP) consortium. From this longitudinal clinical sample we included individuals who had T1-weighted magnetic resonance imaging (MRI) scan acquisitions at baseline and follow-up. Two identical scanners were used and all included participants had their baseline and follow-up scan/s acquired on the same scanner. Detailed information regarding diagnostic criteria, clinical assessments, MRI acquisition and image quality control assessment of the Utrecht Schizophrenia project and the GROUP consortium are described in (Hulshoff Pol et al., 2001; Korver et al., 2012; Kubota et al., 2015; Janssen et al., 2021). Additional

demographic, cognitive, and clinical characteristics of the longitudinal clinical sample are provided in Table A. All participants provided informed consent. Subject recruitment procedures and informed consent forms, including consent to share de-identified data, were approved by the corresponding institutional review board where data were collected.

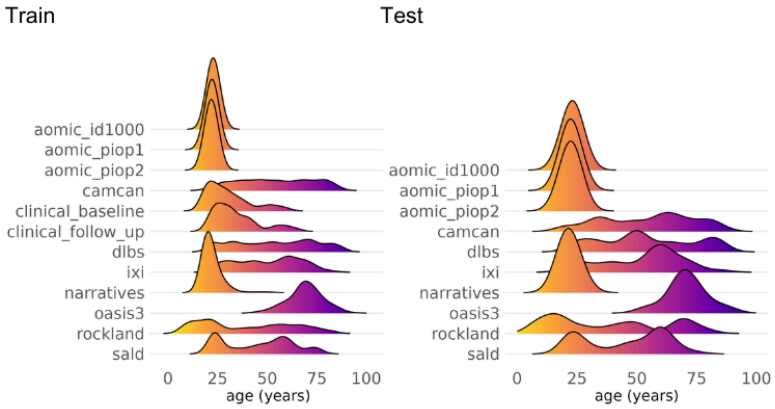

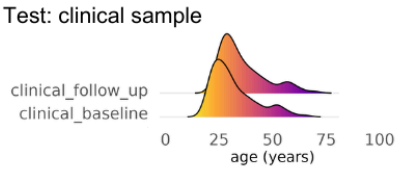

Site	N (subjects)	Age (mean years (SD))	Sex (%F)
aomic_id1000	927	22.85 (1.71)	52.1
aomic_piop1	209	22.18 (1.80)	57.4
aomic_piop2	224	21.96 (1.79)	57.1
camcan	645	54.53 (18.48)	50.9
dlbs	309	54.09 (19.91)	62.1
ixi	456	50.82 (16.15)	56.1
narratives	336	21.92 (4.66)	58.9
oasis3	615	69.44 (8.75)	59.7
rockland	495	39.70 (22.96)	66.1
sald	494	45.18 (17.44)	62.1
clinical_baseline	459	30.24 (10.43)	36.6
clinical_follow_up	459	34.25 (10.71)	36.6

Figure A. Eleven datasets were used in the study. Ten datasets are cross-sectional, publicly available and either include healthy individuals only or only healthy individuals from the dataset were included for the current study. For each of these ten datasets, 90% of individuals were included in the training set and 10% were part of the test set. One longitudinal clinical dataset (utrecht) included healthy controls and individuals with chronic schizophrenia. Of the healthy controls belonging to the longitudinal clinical dataset, 20% were included in the training set and 80% in the test set. All of the individuals with schizophrenia were included in the test set. The age distribution for each dataset within the training/test samples is shown. The table shows the descriptives per dataset. N, number of subjects.

	Healthy		Schizophrenia	
	Baseline (N=292)	Follow-up (N=292)	Baseline (N=167)	Follow-up (N=167)
Age (years)	30.44 (11.02)	34.39 (11.31)	29.90 (9.31)	34.02 (9.60)
Sex (N, (%F))	130 (44.5)		38 (22.8)	
Education (years)	21.92 (25.33)		20.31 (25.84)	
IQ total	110.28 (15.79)	113.89 (16.65)	97.82 (16.60)	103.13 (20.34)
Time between scans (years)	3.95 (1.03)		4.11 (0.95)	
Age of onset (years)			22.14 (5.28)	
Illness duration at scan (years)			6.41 (6.66)	11.08 (7.72)
PANSS total			63.22 (19.38)	50.17 (14.28)
Total Positive			14.91 (5.85)	12.38 (4.65)
Total Negative			16.25 (6.25)	12.83 (5.66)
Total General			31.15 (11.26)	24.97 (7.04)

Table A. Demographic, cognitive, imaging and clinical characteristics of the clinical dataset. All descriptors are mean (standard deviation) unless otherwise noted. N, number of subjects; F, female; PANSS, Positive and Negative Syndrome Scale (Kay et al., 1987).

Image processing and quality control

All T1-weighted images from all datasets were processed centrally using the FreeSurfer analysis suite (v7.1) with default settings (Fischl, 2012). Estimates of 1) cortical volume, 2) surface area, 3) average cortical thickness, 4) average curvature and 5) Gaussian curvature were calculated for each region of the Desikan-Killany-Tourneville (DKT) atlas (Klein and Tourville, 2012). The Freesurfer Euler number was extracted as a proxy for image quality (Rosen et al., 2018).

Subjects were removed if the maximum, absolute, within-dataset centered Euler number was larger than 10 (Rutherford et al., 2023).

Morphometric similarity

A visual overview of the study is given in Figure B. Morphometric similarity was calculated following a previously published protocol (Seidlitz et al., 2018). For each individual and cortical region, cortical volume, surface area, average cortical thickness, average curvature and Gaussian curvature (see Figure B-B) was mean-centered and scaled to account for the different scales of these features. The Pearson coefficient for each pair of resulting 5x1 vectors for all regions of both hemispheres constitute the 62 regions x 62 regions pairwise correlation matrix for each subject. Correlations of each region with all other regions (i.e. the columns of the matrix) were then averaged to obtain mean morphometric similarity values for each region.

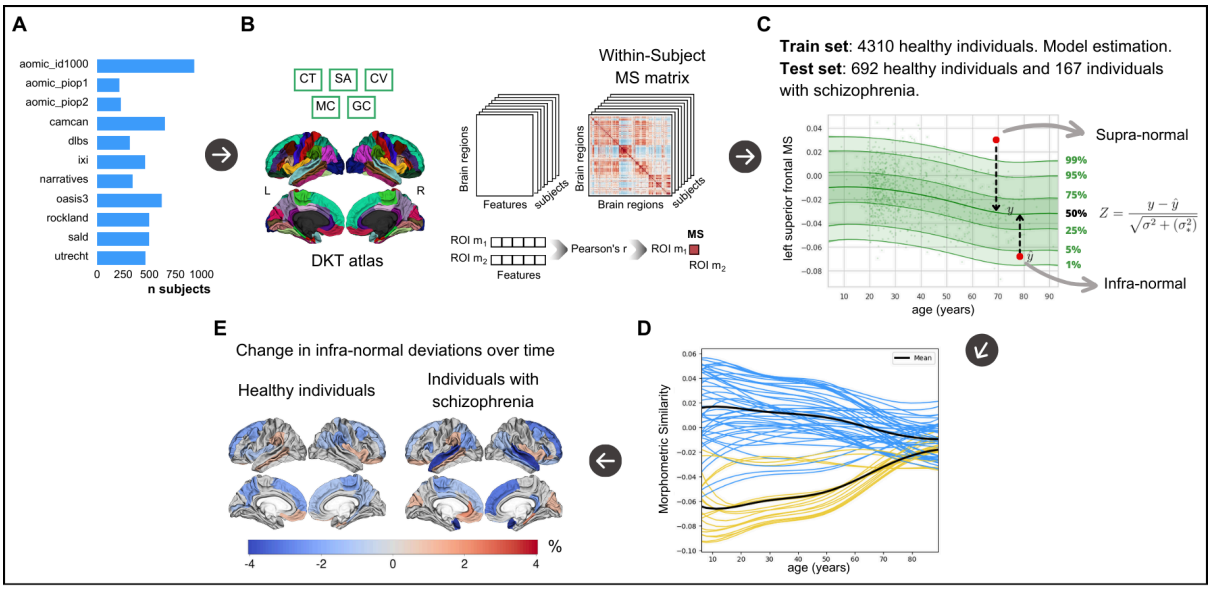

Figure B. Study overview. **A**. Ten cross-sectional datasets consisting of healthy individuals only and one longitudinal dataset consisting of healthy controls and individuals with chronic schizophrenia (utrecht) were used in the study. **B**.

morphometric similarity matrices were constructed following established protocols using five metrics extracted for each cortical region (Seidlitz et al., 2018). **C**. Example centile plot from normative modeling of morphometric similarity of the left hemispheric superior frontal gyrus for assessing individual deviance (Z). Normative modeling was done following established protocols (Rutherford et al., 2022b) using prediction on unseen test data following training of the model. **D**. Normative models for each cortical region morphometric similarity were clustered into groups. **E**. Cortical maps depicting percentage longitudinal change of extreme deviance below the norm, i.e. infra-normal deviance, in individuals with schizophrenia and healthy individuals. n, number of subjects, CT, cortical thickness; SA, surface area; CV, cortical volume; MC, mean curvature; GC, Gaussian curvature. MS, morphometric similarity.

Normative modeling of morphometric similarity

As can be seen in Figure A, for normative modeling, each of the ten datasets containing only healthy controls was split into a training set (90%) and a test set (10%). For the only longitudinal clinical dataset, all individuals with schizophrenia as well as 80% of the healthy controls were included in the test set while the remaining healthy controls (20%) were included in the training set. The per-dataset splits were created using the createDataPartition function from the caret R package, preserving the distribution of age, sex, and scanner (some datasets contained multiple scanners) in both the training and the test split of each dataset. The training set included 4310 participants and the test set 859 participants. Bayesian Linear Regression (BLR) with likelihood warping using a B-spline (spline order=3, number of knots=5) was used to predict morphometric similarity from a vector of covariates

(age, sex, Euler number, and scanner) (Rutherford et al., 2023). For a complete mathematical description and explanation of this implementation, see (Fraza et al., 2021). Briefly, for each brain region of interest (r),

$$y_r = w^T \phi(X) + \epsilon_s \tag{1}$$

where y is the predicted distribution of morphometric similarity for region r, w^T is the estimated weights vector, X is the set of covariates, $\phi(X)$ the B-spline basis expansion applied to them, and ϵ_s a gaussian noise distribution term for scanner *s*.

Individual deviations: infra- and supra-normal morphometric similarity

For each brain region, individuals from the test set were positioned on the normative charts and then categorized as either: (i) normal, i.e. within the normative range of variation for healthy individuals of the same age, sex, Euler number, and scanner; (ii) supra-normal: significantly exceeding the normative range; or, (iii) infra-normal: significantly below the normative range (see Figure A). This mutually exclusive classification was guided by deviation (z) scores quantifying individual deviation from the average. The z-score is calculated for all brain regions (r) and all participants (n) as follows:

$$z_{nr} = \frac{y_{nr} - \widehat{y_{nr}}}{\sqrt{\sigma_r^2 + (\sigma_*^2)_r}} \tag{2}$$

where y_{nr} means the true morphometric similarity value and $\widehat{y}_{nr}$ is the predicted mean morphometric similarity value. The difference in these values is normalized to account for two different sources of variation; σ_r^2 which is the aleatoric uncertainty and reflects the variation between individuals across the population. The epistemic

uncertainty, σ^2_{*r}, accounts for the variance associated to modeling uncertainty introduced by the model assumptions or parameter selection (associated to the age gaps in which there is low density of individuals). As per previous studies (Bethlehem et al., 2020; Janssen et al., 2021; Lv et al., 2021; Di Biase et al., 2022; Rutherford et al., 2023; ENIGMA Clinical High Risk for Psychosis Working Group et al., 2024; Huang et al., 2024) we considered a z-score ≧ than 1.96 as supra-normal and a z-score ≦ -1.96 as infra-normal.

Evaluation of the normative model

The unseen data in the complete test set was used to evaluate the normative model. The evaluation included Q-Q plots, and the metrics proportion of explained variance, mean standardized log loss, standardized mean square error, root mean square error, rho, bayesian information criterion, skewness, and kurtosis (see Supplemental Figure A).

Mapping the DKT atlas regions to functional networks

We focused on seven networks derived from an analysis of an independent resting state fMRI dataset (Thomas Yeo et al., 2011). To obtain a correspondence between the regions of the DKT atlas and the seven functional networks we followed the approach by (Váša et al., 2018). Briefly, for each region of the DKT atlas we calculated the overlap (as the number of vertices) with each of the seven functional networks. Thereafter, for each region, the largest overlap determined to which functional network an region was ascribed. Thus, this resulted in a mapping of each region to one of the seven functional networks. In order to assess deviance of

morphometric similarity for the seven functional networks we averaged the z-scores across regions belonging to each functional network.

Statistical analyses

Clustering of brain regions based on normative models of MS

Normative modeling allowed us to assess whether the age-dependency of normative morphometric similarity was heterogeneous across cortical regions. We tested whether the regions could be clustered into distinct groups of regions based on the age-dependence of MS. We therefore binned the training set along the age range into 27 equally-sized age bins (3.6 years/bin). Thereafter, a 62x27 matrix was constructed where each row was a region and each column contained the median normative morphometric similarity (50th percentile) of a particular age bin. Principal Component Analysis was applied to the matrix using the prcomp R package. The resulting Euclidean distance matrix was used for hierarchical clustering. The optimal number of clusters was determined using the NbClust R package, which generates 23 cluster solutions using different methods and from which the optimal number of clusters is chosen by majority voting (Charrad et al., 2014).

Effects of diagnosis on morphometric similarity based on normative models or 'raw' values

Averaged z-scores of the seven functional networks were compared between healthy controls and individuals with schizophrenia from the longitudinal clinical sample using Welch t-tests. To test whether using z-scores from normative modeling led to stronger diagnostic group results as compared to using 'raw' morphometric similarity (i.e., the traditional approach) we also averaged 'raw' morphometric

similarity across the regions belonging to each of the functional networks. To investigate the diagnostic differences of 'raw' morphometric similarity scores for each functional network, we used seven separate generalized additive models (one for each functional network) to residualize the 'raw' morphometric similarity for age (included as a smooth term to allow for the potentially non-linear association between morphometric similarity and age), sex, Euler number, and scanner (Wood, SN, 2006). For the diagnostic comparison of the residualized 'raw' morphometric similarity we used Welch t-tests. Effect sizes are given as Cohen's d. Only P values that survived FDR correction for multiple comparisons were considered significant.

The percentage of individuals with infra- or supra-normal deviance

We calculated for each region (r) and at each timepoint (*t* = *t*1 or *t*2) the percentage of patients and healthy controls that had supra- or infra-normal z-scores:

$$percentage\ outliers_r(t) = \frac{\sum_{n=1}^{N_{total}} \delta_{rn}(t)}{N_{total_t}} \cdot 100\% \quad (3)$$

where $\delta_{rn}(t)$ equals 1 if participant n=1,...,N_{total} has |Z| > 1.96 in region r at time point *t*, and equals 0 otherwise and N_{total} is the total number of participants at time point *t*. Group differences for each region and at each time point in the proportion of individuals with supra- or infra-normal z-scores were examined using the two-proportions z-test.

Longitudinal differences in percentage of outliers are calculated by subtracting the baseline percentage from the follow-up percentage for each region r:

$$change\ in\ outlier\ percentage_r(t) = percentage\ outliers_r(t2) - percentage\ outliers_r(t1) \quad (4)$$

To assess the spatial distribution of infra- and supra-normal deviations we built diagnostic-wise brain maps (see Figure B-E).

Regional change in outlier count

While the previous analysis focused on outlier participants here we determine the change in total number of outlier regions per participant over time as follows:

$$change\ in\ outlier\ count_n(t) = \sum_{r=1}^{62} \delta_{rn}(t1) - \sum_{r=1}^{62} \delta_{rn}(t2) \quad (5)$$

where δ equals 1 if participant n has |Z| > 1.96 for region r=1,...,62, and equals 0 otherwise. Diagnostic group differences in the change in total number of outlier regions were examined using a Welch t-test. In the group of individuals with schizophrenia we tested for associations between change in outlier count, IQ and PANSS positive, negative and general scores using Pearson correlation.

Sensitivity analyses

We conducted a number of sensitivity analyses. Firstly, we assessed the replicability of morphometric similarity. For all healthy controls of the clinical sample at baseline we calculated the average morphometric similarity for all regions of the atlas that was used in Morgan et al. (2019). We then used a spatial permutation test, the spin test, to correlate our 5-features morphometric similarity map with the publicly available 7-features map from Morgan et al. (2019) (Váša et al., 2018; Morgan et al., 2019). The spin-test provides a P-value derived from a spherical permutation (P_{perm}), obtained by comparing the empirical Spearman's ρ to a null distribution of 10,000 Spearman correlations, between our 5-features map and the randomly rotated projections of the map by Morgan et al. (2019) (Váša et al., 2018). The empirical Spearman's ρ for the correlation between our 5-features map and the 7-features

morphometric similarity map by Morgan et al. (2019) for healthy controls was 0.8 (P_{perm}<0.001) indicating good correspondence between our 5-features map and the 7-features map from (Morgan et al., 2019) (see the 5- and 7-features maps at Supplemental Figure B-A and B-B). To address the effect of scanner harmonization on replicability we repeated the replicability-analysis using COMBAT-corrected input (see Supplemental Figure B-C) (Fortin et al., 2018). Secondly, we repeated the analysis of clustering of regions based on normative models for males and females separately to assess whether results differed per sex (see Supplemental Figure C). Thirdly, we averaged morphometric similarity across all regions and hemispheres to determine whole brain morphometric similarity and compared these between groups (see Supplemental Figure D).

Results

Visualization and evaluation of the normative models

An exemplary normative model plot with percentile curves for the left hemispheric superior frontal gyrus can be seen in Figure B-C. Evaluation metrics of the normative models can be found in Supplemental Figure A.

Clustering of brain regions based on normative models of MS

The first two principal components explained 98.63% of the variance (1st component: R^2=77.14%, 2nd component: R^2=21.49%) of the median normative morphometric similarity across age groups and were therefore selected for constructing the distance matrix (see Figure C). Clustering gave two clusters as the optimal solution. As can be seen in Figure C, clustering was extremely similar between left and right hemispheres. The first cluster (number of regions = 44, 71% of all regions) includes mostly frontal and temporal regions with positive morphometric similarity tending towards zero during aging. The second cluster (18 regions, 29%) consists of inferior prefrontal, postcentral gyrus and occipital regions with negative morphometric similarity tending towards zero during aging.

39% of all regions from cluster 1 were part of the default mode network as defined by Yeo et al. (2011) which is significantly more than expected ($P<0.001$, one sample z-test for proportions, see Table B). For cluster 2 this was 11% ($P=0.48$).

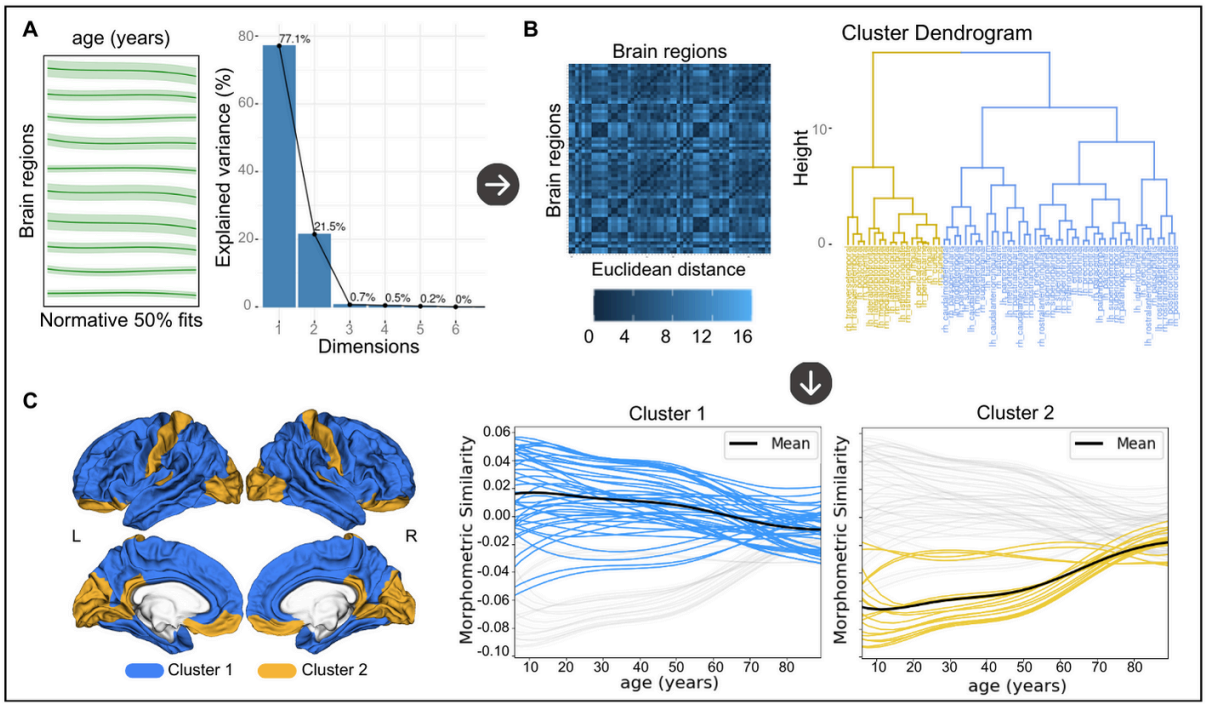

Figure C. Clustering of brain regions based on normative modeling of morphometric similarity. **A**. The median normative morphometric similarity of the normative model of each cortical region was entered into a Principal Component Analysis (PCA). The first two components explaining 98.6% of the variance were selected. **B**. The Euclidean distance matrix was extracted from the PCA output and used for hierarchical clustering. A two cluster solution was determined optimal. **C**. Each plot shows the median normative fits for a cluster with the remaining normative fits in gray. The average fit across all fits belonging to a cluster is added in black. The cluster solution was also visualized on the cortex displaying the distribution of the two clusters across the cortex. L, left hemisphere, R, right hemisphere. The upper row are lateral views, the bottom row are medial views.

Network	MS Cluster 1	MS Cluster 2
Visual	2	6
Somato Motor	2	2
Dorsal Attention	4	4
Ventral Attention	8	0
Limbic	9	0
Fronto Parietal	2	4
Default Mode	17	2

Table B. Number of regions from each of the two clusters belonging to each of the seven functional networks as defined by Yeo et al. (2011) (Thomas Yeo et al., 2011). MS, morphometric similarity.

Effects of diagnosis on morphometric similarity using normative models or 'raw' values

At baseline, the group of individuals with schizophrenia had a positive average deviance of morphometric similarity for the somatosensory network which differed significantly from the negative average deviance of morphometric similarity in healthy controls ($d=0.30$; $p<0.01$). Individuals with schizophrenia had a negative average deviance of morphometric similarity for the default mode network as defined by Yeo et al. (2011) which differed significantly from the positive average deviance of morphometric similarity in healthy controls ($d=-0.36$; $p<0.001$), see Table C and Figure D. At follow-up, the group of individuals with schizophrenia maintained the negative morphometric similarity for the default mode network as defined by Yeo et al. (2011) compared to healthy controls but this difference with healthy controls did

not withstand correction for multiple comparisons. With respect to the ‘raw’ values, there was lower average deviance morphometric similarity for the default mode network as defined by Yeo et al. (2011) for the group of individuals with schizophrenia compared to healthy controls but with a smaller effect size compared to the normative-modeling based z-scores ($d=-0.27$, $p<0.01$) at baseline, (see Table C and Figure D).

Timepoint	Network	z-scores		Mean MS			
		t-statistic	$P\ value^A$	$mean\ (SD)_H$	$mean\ (SD)_{SZ}$	t-statistic	$P\ value^A$
Baseline	Visual	1.451	0.148	-0.021 (0.007)	-0.02 (0.007)	1.764	0.022
	Somato Motor	2.940	0.003*	-0.015 (0.018)	-0.012 (0.017)	1.011	0.313
	Dorsal Attention	-0.844	0.399	-0.018 (0.009)	-0.018 (0.009)	-0.199	0.842
	Ventral Attention	-0.075	0.940	-0.017 (0.007)	-0.017 (0.008)	1.162	0.246
	Limbic	-1.902	0.058	-0.013 (0.01)	-0.014 (0.011)	-0.778	0.437
	Fronto Parietal	-0.805	0.421	-0.005 (0.013)	-0.006 (0.013)	-1.461	0.145
	Default Mode	-3.665	0.0002 *	-0.008 (0.007)	-0.01 (0.006)	-2.753	0.006*
Follow-up	Visual	1.519	0.130	-0.022 (0.007)	-0.02 (0.007)	1.721	0.216
	Somato Motor	1.675	0.095	-0.018 (0.018)	-0.017 (0.018)	0.461	0.645
	Dorsal Attention	-0.867	0.387	-0.017 (0.009)	-0.017 (0.009)	-0.322	0.748
	Ventral Attention	-0.819	0.413	-0.016 (0.008)	-0.017 (0.007)	-1.080	0.281
	Limbic	-0.617	0.537	-0.012 (0.011)	-0.012 (0.011)	0.256	0.798
	Fronto Parietal	-0.361	0.718	-0.006 (0.015)	-0.007 (0.013)	-0.823	0.411
	Default Mode	-2.046	0.041	-0.008 (0.007)	-0.009 (0.006)	-1.495	0.136

Table C. Results of statistical tests for case-control differences in z-scores and 'raw' (i.e. traditional values rather than normative modeling-based z-scores) morphometric

similarity averaged across regions belonging to the seven functional brain networks as identified by Yeo et al. (2011) (Thomas Yeo et al., 2011). A positive t-statistic indicates that the group of individuals with schizophrenia has a higher mean than the group of healthy controls while a negative t-statistic indicates that the group of individuals with schizophrenia has a lower mean than the group of healthy controls. ^{A}P values with an asterisk survive multiple comparisons correction. MS, morphometric similarity. H, healthy controls, SZ, schizophrenia.

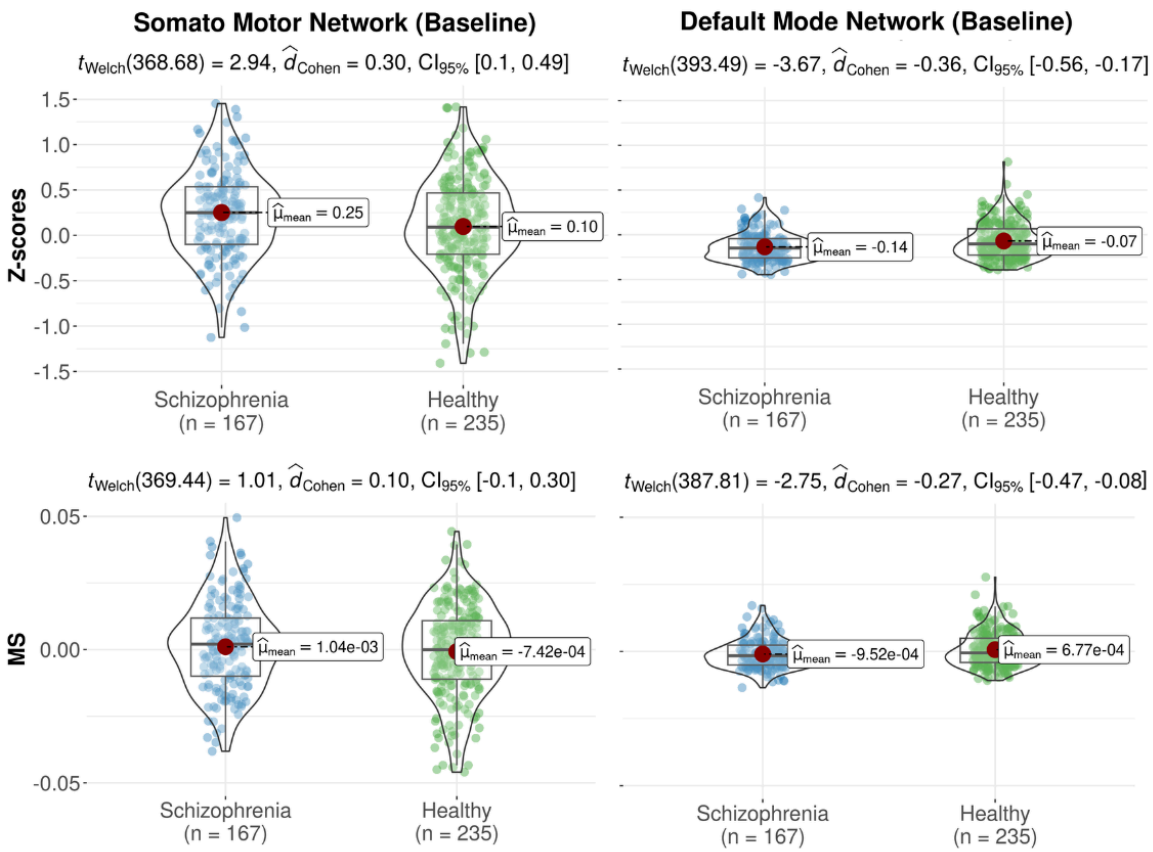

Figure D. Violin plots of significant (FDR-corrected) differences in z-scores and 'raw' morphometric similarity (i.e. traditional values rather than normative modeling-based z-scores) of two functional networks between the group of healthy controls and the group of individuals with schizophrenia. MS, morphometric similarity.

The percentage of individuals with infra- or supra-normal deviance per region

The percentage of participants, regardless of the diagnostic category, with either infra- or supra-normal deviance was low at baseline and follow-up (see Figure E-A and E-B). Across both timepoints and regions, for individuals with schizophrenia the percentage infra-normal regional morphometric similarity z-scores ranged between 0 and 6.0% and for healthy controls it ranged between 0 and 4.3%; the corresponding range for the percentages of supra-normal morphometric similarity z-scores were 0–5.4% and 0–6.0%, respectively. There were no significant diagnostic differences in the percentage of participants with infra- or supra-normal regional values at baseline and follow-up ($P>0.05$).

At baseline and follow-up, the percentages of individuals with schizophrenia with infra-normal deviance were highest in the superior temporal and superior frontal regions. For both diagnostic groups, the percentages of participants with supra-normal deviance were highest in the occipital lobe and postcentral gyrus (see Figure E-A and E-B).

With respect to changes over time, we calculated the change over time in the regional percentage of infra- and supra-normal deviance. In both diagnostic groups and for most regions the change in percentage was generally more negative for infra-normal deviance compared to supra-normal deviance (see Figure E-C). This indicated that for most regions, ‘normalizing’ of participants over time occurred more frequently for those that had infra-normal deviance compared to those that had supra-normal deviance. In other words, having infra-normal deviance for a region increased a participant’s probability of normalizing during follow-up compared to having supra-normal deviance. For infra-normal deviance the regions with highest percentages of change were the bilateral superior temporal and left superior and

medial frontal regions with a decrease over time of 4.2%, 0.6% and 1.8%, respectively. For supra-normal deviance the region with the highest percentage of change was the left postcentral gyrus with an increase of 1.2% (see Figure E-C).

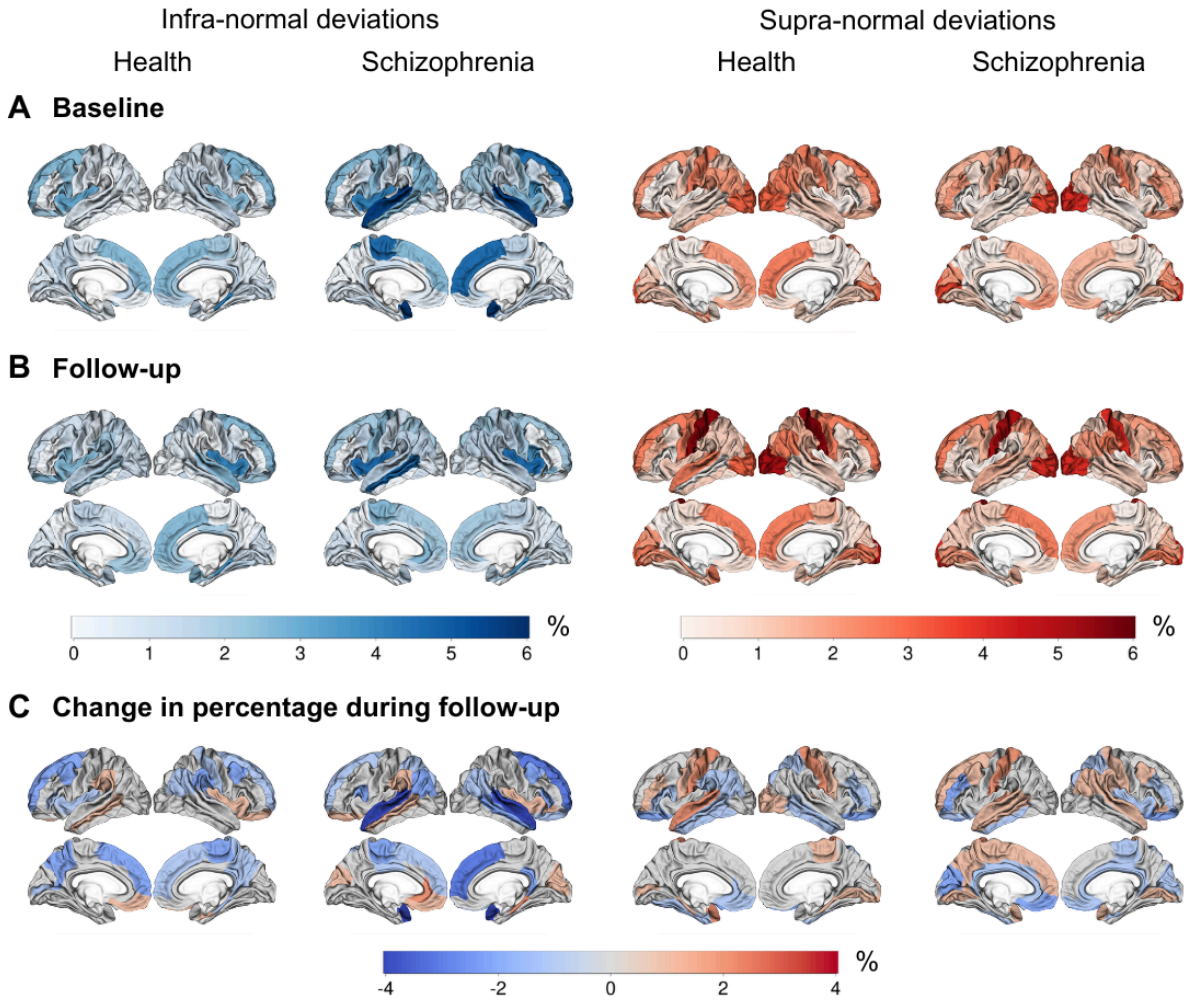

Figure E. Cortical maps showing the percentage of individuals with infra- and supra-deviance morphometric similarity per region, **A**) at baseline, **B**) at follow-up, and **C**) the change in percentage during follow-up (i.e., percentage at follow-up - percentage at baseline). A negative percentage means that the regional percentage of infra- or supra-normal deviance decreased during follow-up.

Regional change in outlier count

No significant group differences between healthy controls and individuals with schizophrenia were found for the average longitudinal change in total outlier regions (see Supplemental Figure E). In the group of individuals with schizophrenia no significant correlations were found between cross-sectional and longitudinal total outlier count and IQ and PANSS scores ($P_{fdr}>0.05$).

Discussion

This investigation is the first, to the best of our knowledge, to integrate longitudinal assessments of morphometric similarity, a relatively recent multivariate neuroimaging characteristic implicated in psychosis, with normative modeling.

We established regional age-dependent normative trajectories for morphometric similarity across the adult age range. We found that in general mean regional morphometric similarity converged towards zero with increasing age which is coherent with a prior study (Zhukovsky et al., 2022). Here, we extended prior findings by showing that age-dependent trajectories can be clustered into two groups. One cluster contains trajectories that start with positive morphometric similarity at younger ages which decrease to zero with age. The other cluster starts with negative morphometric similarity which decreases to zero with age. We also showed that the default mode network, as defined by Yeo et al. (2011), contained disproportionally more regions of the former compared to the latter cluster. Studies have consistently reported age-related reductions in resting-state functional connectivity of the default mode network as well as structural network connectivity (Geerligs et al., 2015; Cox et al., 2016). As such, these findings are coherent with our observed decline of morphometric similarity across a large age range, the notion that to a certain degree brain structure underlies function and provides support for our normative models (Zhukovsky et al., 2022; Pang et al., 2023).

Our investigation aimed to compare morphometric similarity across functional networks between individuals with schizophrenia and healthy subjects. Our findings revealed that, at baseline, individuals diagnosed with schizophrenia exhibited increased morphometric similarity across regions pertaining to the somato-motor network and decreased morphometric similarity across regions pertaining to the

default mode network when compared to the healthy control subjects. The reduced morphometric similarity in the group of individuals with chronic schizophrenia aligns with previous research findings in early-onset and chronic schizophrenia (Morgan et al., 2019; Yao et al., 2023). A recent study demonstrated that morphometric similarity was positively correlated with the likelihood of cellular network structures forming axonal connections (Lin et al., 2024). In schizophrenia, axonal dysconnectivity between networks might lead to the micro-structural and functional connectivity deficits observed across various age groups affected by the disease, including children, adolescents, and adults (Kelly et al., 2018; Heuvel and Sporns, 2019; Barth et al., 2023).

The increased morphometric similarity observed in the somatomotor network poses a complex challenge for explanation, considering the general neglect of the somatomotor network within psychiatric models of schizophrenia. Nonetheless, a recent resting-state fMRI study shed light on altered somatomotor network connectivity, suggesting its potential relevance across various psychiatric disorders, associating it with psychopathology, cognitive impairment, and impulsivity (Kebets et al., 2019).

In a minority of individuals with schizophrenia, infra-normal and supra-normal deviations of morphometric similarity were present (<6%), mirroring observations akin to those found in healthy individuals. Notably, outlier percentages did not differ significantly between baseline and follow-up assessments. These results indicate that variations in morphometric similarity among individuals with schizophrenia predominantly existed within the spectrum of variations observed in the healthy reference sample (Wolfers et al., 2018; Winter et al., 2022; Bedford et al., 2023; Segal et al., 2023; ENIGMA Clinical High Risk for Psychosis Working Group et al.,

2024). Previous normative modeling studies conducted on individuals with schizophrenia or those at high risk for the condition have reported similar percentages for cortical volume and cortical thickness (Wolfers et al., 2018; Segal et al., 2023; ENIGMA Clinical High Risk for Psychosis Working Group et al., 2024). Notably, the majority of these studies failed to establish a relationship between z-scores and the severity of symptomatology.

Our study involved a comparison between the output features derived from normative modeling, specifically deviation scores, and the 'raw' or traditional features during univariate group difference testing between individuals with schizophrenia and control subjects. The findings demonstrated potential advantages in utilizing deviation scores over traditional features across all group comparisons. Using normative models we replicated prior findings of altered morphometric similarity in psychotic disorders and when applied to the same data, normative model-based results provided increased statistical significance when compared to raw data models. Our results underscore that normative modeling possesses the capacity to capture overarching population patterns, discern clinical disparities between groups, and retain the ability to investigate individual differences (Rutherford et al., 2023). One reason why normative models may show enhanced performance compared to raw data models is that normative modeling allows for the consideration of numerous sources of variance. Some of these sources may not carry clinical significance (e.g., scanner variability), while others simultaneously encapsulate clinically relevant information within the framework of a reference cohort. The utility of the normative model extends beyond the mere elimination of the effects of confounding factors such as scanner noise. This is evident as our findings indicate that even after removing nuisance covariates (age, sex, scanner, Euler number) from the raw data,

the features derived from normative modeling continue to exhibit superior performance (Rutherford et al., 2022a, 2023).

We demonstrated significant heterogeneity in morphometric similarity among individuals with schizophrenia, suggesting that structural deficits in schizophrenia are nuanced and intricate, which contributes to a substantial overlap between individuals with chronic schizophrenia and healthy controls. Similar observations have been reported for other structural phenotypes, implying that structural MRI-derived phenotypes, including morphometric similarity, may have restricted utility in elucidating the pathophysiology of schizophrenia (Winter et al., 2022).

For clinical translation, progressions in normative modeling stand as a crucial prerequisite, underscoring the necessity for a broadened diversification of datasets. While the present study benefited from a substantial training set, larger and more heterogeneous datasets, incorporating not solely European ancestry data, emerge as imperative for heightened performance and validity (Bethlehem et al., 2022). Additionally, the acquisition of longitudinal data may introduce supplementary noise, mandating test-retest reliability investigations to effectively model such noise alongside tailored modeling methodologies (Di Biase et al., 2023). The adoption of specialized processing pipelines tailored to longitudinal data may further alleviate noise (Thompson et al., 2011). Lastly, the normative modeling framework employed herein treats each region as independent, notwithstanding potential correlations among z-scores from neighboring regions. To mitigate this challenge, one plausible strategy involves implementing data reduction techniques, such as principal component analysis applied to the z-scores (Rutherford et al., 2022b). While our sample size of individuals with schizophrenia was comparable to previous normative modeling studies, its application to larger (multicenter) clinical samples may enable

the identification of distinct clusters of patients exhibiting significant deviance (Wolfers et al., 2018; Rutherford et al., 2023). Furthermore, despite the comprehensive characterization of the sample through diagnostic, clinical, and cognitive assessments conducted by experienced professionals, information regarding development or premorbid adjustment was unavailable.

In conclusion, the current study finds decreased average morphometric similarity of the default mode network in a group of individuals with chronic schizophrenia, replicating previous findings in groups of individuals with first-episode psychosis. However, reductions are only present in a minority of individuals with schizophrenia indicating that caution is warranted when extrapolating group-average results to the individual.

References

Alnæs D et al. (2019) Brain Heterogeneity in Schizophrenia and Its Association With Polygenic Risk. JAMA Psychiatry 76:739–748.

Barbora Rehák Bučková, Charlotte Fraza, Rastislav Rehák, Marián Kolenič, Christian Beckmann, Filip Španiel, Andre Marquand, Jaroslav Hlinka (2024) Using normative models pre-trained on cross-sectional data to evaluate longitudinal changes in neuroimaging data. bioRxiv:2023.06.09.544217.

Barth C et al. (2023) In vivo white matter microstructure in adolescents with early-onset psychosis: a multi-site mega-analysis. Mol Psychiatry 28:1159–1169.

Bedford SA et al. (2023) Brain-charting autism and attention deficit hyperactivity disorder reveals distinct and overlapping neurobiology. MedRxiv Prepr Serv Health Sci:2023.12.06.23299587.

Bethlehem R a. I et al. (2022) Brain charts for the human lifespan. Nature 604:525–533.

Bethlehem RAI, Seidlitz J, Romero-Garcia R, Trakoshis S, Dumas G, Lombardo MV (2020) A normative modelling approach reveals age-atypical cortical thickness in a subgroup of males with autism spectrum disorder. Commun Biol 3:486.

Broyd SJ, Demanuele C, Debener S, Helps SK, James CJ, Sonuga-Barke EJS (2009) Default-mode brain dysfunction in mental disorders: a systematic review. Neurosci Biobehav Rev 33:279–296.

Brugger SP, Howes OD (2017) Heterogeneity and Homogeneity of Regional Brain Structure in Schizophrenia: A Meta-analysis. JAMA Psychiatry 74:1104–1111.

Charrad M, Ghazzali N, Boiteau V, Niknafs A (2014) NbClust: An R Package for Determining the Relevant Number of Clusters in a Data Set. J Stat Softw 61:1–36.

Cox SR, Ritchie SJ, Tucker-Drob EM, Liewald DC, Hagenaars SP, Davies G, Wardlaw JM, Gale CR, Bastin ME, Deary IJ (2016) Ageing and brain white matter structure in 3,513 UK Biobank participants. Nat Commun 7:13629.

Di Biase MA et al. (2022) Cell type-specific manifestations of cortical thickness heterogeneity in schizophrenia. Mol Psychiatry 27:2052–2060.

Di Biase MA, Tian YE, Bethlehem RAI, Seidlitz J, Alexander-Bloch AF, Yeo BTT, Zalesky A (2023) Mapping human brain charts cross-sectionally and longitudinally. Proc Natl Acad Sci U S A 120:e2216798120.

ENIGMA Clinical High Risk for Psychosis Working Group et al. (2024) Normative Modeling of Brain Morphometry in Clinical High Risk for Psychosis. JAMA Psychiatry 81:77–88.

Fischl B (2012) FreeSurfer. NeuroImage 62:774–781.

Fortin J-P, Cullen N, Sheline YI, Taylor WD, Aselcioglu I, Cook PA, Adams P, Cooper C, Fava M, McGrath PJ, McInnis M, Phillips ML, Trivedi MH, Weissman MM, Shinohara RT (2018) Harmonization of cortical thickness measurements across scanners and sites. NeuroImage 167:104–120.

Fraza CJ, Dinga R, Beckmann CF, Marquand AF (2021) Warped Bayesian linear regression for normative modelling of big data. NeuroImage 245:118715.

Geerligs L, Renken RJ, Saliasi E, Maurits NM, Lorist MM (2015) A Brain-Wide Study of Age-Related Changes in Functional Connectivity. Cereb Cortex N Y N 1991 25:1987–1999.

Haijma SV, Van Haren N, Cahn W, Koolschijn PCMP, Hulshoff Pol HE, Kahn RS (2013) Brain volumes in schizophrenia: a meta-analysis in over 18 000 subjects. Schizophr Bull 39:1129–1138.

Heuvel MP van den, Sporns O (2019) A cross-disorder connectome landscape of brain dysconnectivity. Nat Rev Neurosci 20:435.

Huang AS, Kang K, Vandekar S, Rogers BP, Heckers S, Woodward ND (2024) Lifespan development of thalamic nuclei and characterizing thalamic nuclei abnormalities in schizophrenia using normative modeling. Neuropsychopharmacol Off Publ Am Coll Neuropsychopharmacol.

Hulshoff Pol HE, Schnack HG, Mandl RC, van Haren NE, Koning H, Collins DL, Evans AC, Kahn RS (2001) Focal gray matter density changes in schizophrenia. Arch Gen Psychiatry 58:1118–1125.
Janssen J, Díaz-Caneja CM, Alloza C, Schippers A, de Hoyos L, Santonja J, Gordaliza PM, Buimer EEL, van Haren NEM, Cahn W, Arango C, Kahn RS, Hulshoff Pol HE, Schnack HG (2021) Dissimilarity in Sulcal Width Patterns in the Cortex can be Used to Identify Patients With Schizophrenia With Extreme Deficits in Cognitive Performance. Schizophr Bull 47:552–561.
Kay SR, Fiszbein A, Opler LA (1987) The positive and negative syndrome scale (PANSS) for schizophrenia. Schizophr Bull 13:261–276.
Kebets V, Holmes AJ, Orban C, Tang S, Li J, Sun N, Kong R, Poldrack RA, Yeo BTT (2019) Somatosensory-Motor Dysconnectivity Spans Multiple Transdiagnostic Dimensions of Psychopathology. Biol Psychiatry 86:779–791.
Kelly S et al. (2018) Widespread white matter microstructural differences in schizophrenia across 4322 individuals: results from the ENIGMA Schizophrenia DTI Working Group. Mol Psychiatry 23:1261–1269.
Klein A, Tourville J (2012) 101 labeled brain images and a consistent human cortical labeling protocol. Front Neurosci 6:171.
Korver N, Quee PJ, Boos HBM, Simons CJP, de Haan L, GROUP investigators (2012) Genetic Risk and Outcome of Psychosis (GROUP), a multi-site longitudinal cohort study focused on gene-environment interaction: objectives, sample characteristics, recruitment and assessment methods. Int J Methods Psychiatr Res 21:205–221.
Kubota M, van Haren NEM, Haijma SV, Schnack HG, Cahn W, Hulshoff Pol HE, Kahn RS (2015) Association of IQ Changes and Progressive Brain Changes in Patients With Schizophrenia. JAMA Psychiatry 72:803–812.
Lin S, Lv X, Lin X, Chen S, Li Y, Xu M, Qiu Y, Tang L (2024) Modulation Effects of the CEP128 Gene on Radiotherapy-Related Brain Injury: A Longitudinal Structural Study Using Multi-Parametric Brain MR Images. J Magn Reson Imaging JMRI 59:648–658.
Lu H, Xu F, Rodrigue KM, Kennedy KM, Cheng Y, Flicker B, Hebrank AC, Uh J, Park DC (2011) Alterations in cerebral metabolic rate and blood supply across the adult lifespan. Cereb Cortex N Y N 1991 21:1426–1434.
Lv J, Di Biase M, Cash RFH, Cocchi L, Cropley VL, Klauser P, Tian Y, Bayer J, Schmaal L, Cetin-Karayumak S, Rathi Y, Pasternak O, Bousman C, Pantelis C, Calamante F, Zalesky A (2021) Individual deviations from normative models of brain structure in a large cross-sectional schizophrenia cohort. Mol Psychiatry 26:3512–3523.
Marcus DS, Fotenos AF, Csernansky JG, Morris JC, Buckner RL (2010) Open access series of imaging studies: longitudinal MRI data in nondemented and demented older adults. J Cogn Neurosci 22:2677–2684.
Marquand AF, Kia SM, Zabihi M, Wolfers T, Buitelaar JK, Beckmann CF (2019) Conceptualizing mental disorders as deviations from normative functioning. Mol Psychiatry 24:1415–1424.
McGrath J, Saha S, Chant D, Welham J (2008) Schizophrenia: a concise overview of incidence, prevalence, and mortality. Epidemiol Rev 30:67–76.
Morgan SE, Seidlitz J, Whitaker KJ, Romero-Garcia R, Clifton NE, Scarpazza C, van Amelsvoort T, Marcelis M, van Os J, Donohoe G, Mothersill D, Corvin A, Pocklington A, Raznahan A, McGuire P, Vértes PE, Bullmore ET (2019) Cortical patterning of abnormal morphometric similarity in psychosis is associated with brain expression of schizophrenia-related genes. Proc Natl Acad Sci U S A 116:9604–9609.
Nastase SA et al. (2021) The “Narratives” fMRI dataset for evaluating models of naturalistic language comprehension. Sci Data 8:250.
Nooner KB et al. (2012) The NKI-Rockland Sample: A Model for Accelerating the Pace of Discovery Science in Psychiatry. Front Neurosci 6:152.
Pang JC, Aquino KM, Oldehinkel M, Robinson PA, Fulcher BD, Breakspear M, Fornito A (2023) Geometric constraints on human brain function. Nature 618:566–574.
Rosen AFG et al. (2018) Quantitative assessment of structural image quality. NeuroImage

169:407–418.
Rutherford S et al. (2022a) Charting brain growth and aging at high spatial precision. eLife 11:e72904.
Rutherford S, Barkema P, Tso IF, Sripada C, Beckmann CF, Ruhe HG, Marquand AF (2023) Evidence for embracing normative modeling. eLife 12:e85082.
Rutherford S, Kia SM, Wolfers T, Fraza C, Zabihi M, Dinga R, Berthet P, Worker A, Verdi S, Ruhe HG, Beckmann CF, Marquand AF (2022b) The normative modeling framework for computational psychiatry. Nat Protoc 17:1711–1734.
Sebenius I, Seidlitz J, Warrier V, Bethlehem RAI, Alexander-Bloch A, Mallard TT, Garcia RR, Bullmore ET, Morgan SE (2023) Robust estimation of cortical similarity networks from brain MRI. Nat Neurosci 26:1461–1471.
Segal A et al. (2023) Regional, circuit and network heterogeneity of brain abnormalities in psychiatric disorders. Nat Neurosci 26:1613–1629.
Seidlitz J, Váša F, Shinn M, Romero-Garcia R, Whitaker KJ, Vértes PE, Wagstyl K, Kirkpatrick Reardon P, Clasen L, Liu S, Messinger A, Leopold DA, Fonagy P, Dolan RJ, Jones PB, Goodyer IM, NSPN Consortium, Raznahan A, Bullmore ET (2018) Morphometric Similarity Networks Detect Microscale Cortical Organization and Predict Inter-Individual Cognitive Variation. Neuron 97:231-247.e7.
Shafto MA, Tyler LK, Dixon M, Taylor JR, Rowe JB, Cusack R, Calder AJ, Marslen-Wilson WD, Duncan J, Dalgleish T, Henson RN, Brayne C, Matthews FE, Cam-CAN (2014) The Cambridge Centre for Ageing and Neuroscience (Cam-CAN) study protocol: a cross-sectional, lifespan, multidisciplinary examination of healthy cognitive ageing. BMC Neurol 14:204.
Snoek L, van der Miesen MM, Beemsterboer T, van der Leij A, Eigenhuis A, Steven Scholte H (2021) The Amsterdam Open MRI Collection, a set of multimodal MRI datasets for individual difference analyses. Sci Data 8:85.
Thomas Yeo BT, Krienen FM, Sepulcre J, Sabuncu MR, Lashkari D, Hollinshead M, Roffman JL, Smoller JW, Zöllei L, Polimeni JR, Fischl B, Liu H, Buckner RL (2011) The organization of the human cerebral cortex estimated by intrinsic functional connectivity. J Neurophysiol 106:1125–1165.
Thompson WK, Holland D, Alzheimer's Disease Neuroimaging Initiative (2011) Bias in tensor based morphometry Stat-ROI measures may result in unrealistic power estimates. NeuroImage 57:1–4.
van Erp TGM et al. (2018) Cortical Brain Abnormalities in 4474 Individuals With Schizophrenia and 5098 Control Subjects via the Enhancing Neuro Imaging Genetics Through Meta Analysis (ENIGMA) Consortium. Biol Psychiatry 84:644–654.
Váša F, Seidlitz J, Romero-Garcia R, Whitaker KJ, Rosenthal G, Vértes PE, Shinn M, Alexander-Bloch A, Fonagy P, Dolan RJ, Jones PB, Goodyer IM, NSPN consortium, Sporns O, Bullmore ET (2018) Adolescent Tuning of Association Cortex in Human Structural Brain Networks. Cereb Cortex N Y N 1991 28:281–294.
Wei D, Zhuang K, Ai L, Chen Q, Yang W, Liu W, Wang K, Sun J, Qiu J (2018) Structural and functional brain scans from the cross-sectional Southwest University adult lifespan dataset. Sci Data 5:180134.
Winter NR et al. (2022) Quantifying Deviations of Brain Structure and Function in Major Depressive Disorder Across Neuroimaging Modalities. JAMA Psychiatry 79:879–888.
Wolfers T, Doan NT, Kaufmann T, Alnæs D, Moberget T, Agartz I, Buitelaar JK, Ueland T, Melle I, Franke B, Andreassen OA, Beckmann CF, Westlye LT, Marquand AF (2018) Mapping the Heterogeneous Phenotype of Schizophrenia and Bipolar Disorder Using Normative Models. JAMA Psychiatry 75:1146–1155.
Wood, SN (2006) Generalized additive models: an introduction with R. Chapman Hall/CRC.
Yao G, Zou T, Luo J, Hu S, Yang L, Li J, Li X, Zhang Y, Feng K, Xu Y, Liu P (2023) Cortical structural changes of morphometric similarity network in early-onset schizophrenia correlate with specific transcriptional expression patterns. BMC Med 21:479.
Zhukovsky P, Savulich G, Morgan S, Dalley JW, Williams GB, Ersche KD (2022) Morphometric similarity deviations in stimulant use disorder point towards abnormal

brain ageing. Brain Commun 4:fcac079.

Data availability

The study IDs of the included participants from the ten publicly available datasets, the five regional metrics and regional morphometric similarity from the ten publicly available datasets, the overlap between the DKT atlas and the 7 functional networks, the normative model plots with percentile curves, the Q-Q plots, the information and usage instructions about the docker we created for normative modeling are all available at https://github.com/iamjoostjanssen/NormModel_MorphoSim_SZ.

Aomic (id1000, piop1 and piop2) is available at https://openneuro.org/datasets/ds003097, https://openneuro.org/datasets/ds002785 and https://openneuro.org/datasets/ds002790, camcan is available at https://camcan-archive.mrc-cbu.cam.ac.uk, dlbs is available at https://fcon_1000.projects.nitrc.org/indi/retro/dlbs, ixi is available at http://brain-development.org/ixidataset, narratives is available at https://openneuro.org/datasets/ds002345, oasis3 is available at www.oasis-brains.org, rockland is available at http://fcon_1000.projects.nitrc.org/indi/enhanced and sald is available at http://fcon_1000.projects.nitrc.org/indi/retro/sald.

Acknowledgements

This work was supported by the Spanish Ministry of Science, Innovation and Universities. Instituto de Salud Carlos III (PI16/02012, PI17/01249, PI17/00997. PI19/01024), co-financed by ERDF funds from the European Commission, “A way of making Europe”, CIBERSAM, Regional Government (B2017/BMD-3740 AGES-CM-2) and JR19/00024 (Dr. Díaz-Caneja). The authors thank Yasser Alemán-Goméz, Alberto Fernández Pena, Zimbo Boudewijns, and Joyce van Baaren for code and technical assistance.

Disclosures

Dr. Díaz-Caneja has received honoraria from Sanofi-Aventis and Abbvie. Dr. Arango has been a consultant to or has received honoraria or grants from Acadia, Angelini, Gedeon Richter, Janssen-Cilag, Lundbeck, Otsuka, Roche, Sage, Servier, Shire, Schering-Plough, Sumitomo Dainippon Pharma, Sunovion, and Takeda. Dr. Cahn has received unrestricted research grants from or served as an independent symposium speaker or consultant for Eli Lilly, Bristol-Myers Squibb, Lundbeck, Sanofi-Aventis, Janssen-Cilag, AstraZeneca, and Schering-Plough. The other authors report no financial relationships with commercial interests.